



Bethe Center for
Theoretical Physics

10 Years MITP

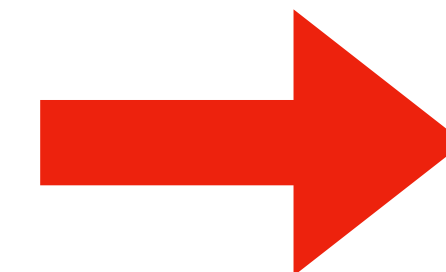
UNIVERSITÄT **BONN**

Light Long-lived Particles

Herbi Dreiner – University of Bonn

Work performed with: Jordy de Vries, Florian Domingo, Julian Günther
Dominik Köhler, Saurabh Nangia, Zeren Simon Wang
Guanghui Zhou

- 10 Years of MITP!
- We have benefitted also greatly in Bonn.
- Have personally been to 5 workshops
- Have sent many students & postdocs to workshops and schools
- **Physik im Theater!**



Physik im Theater - Staatstheater Mainz

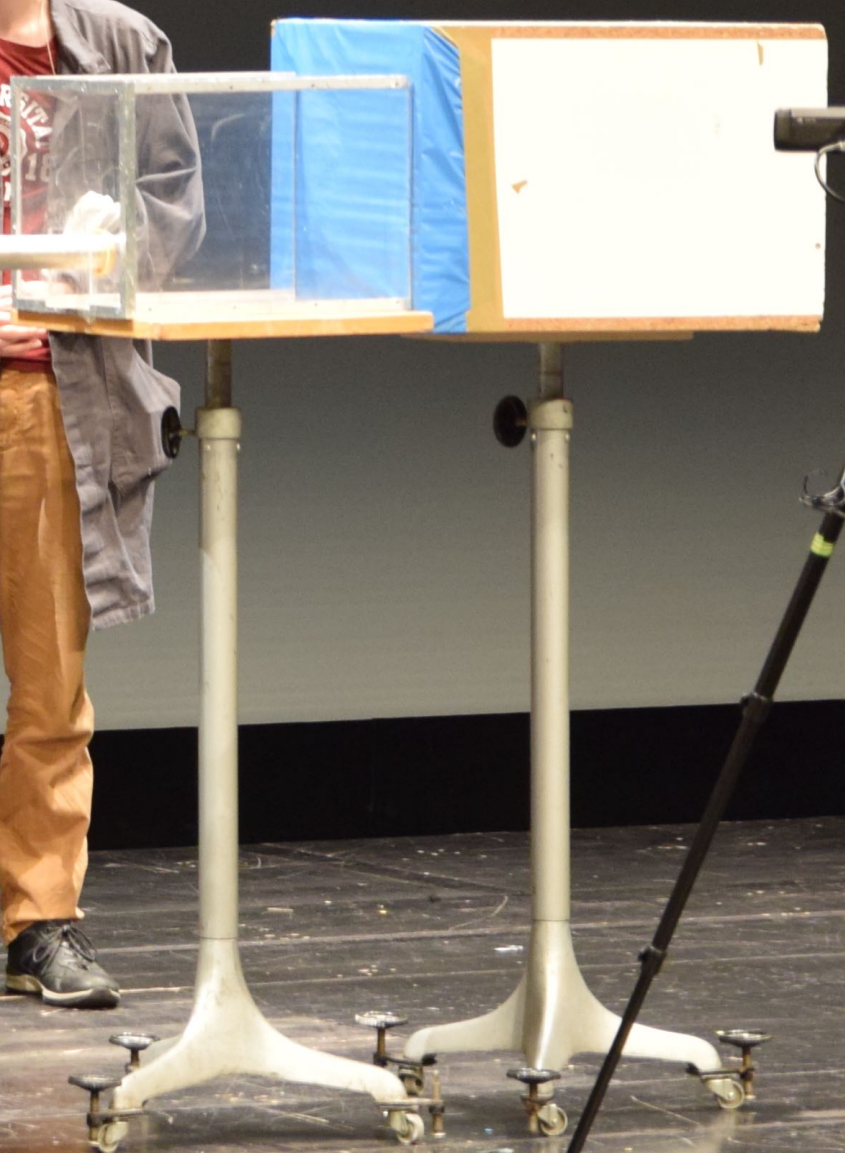
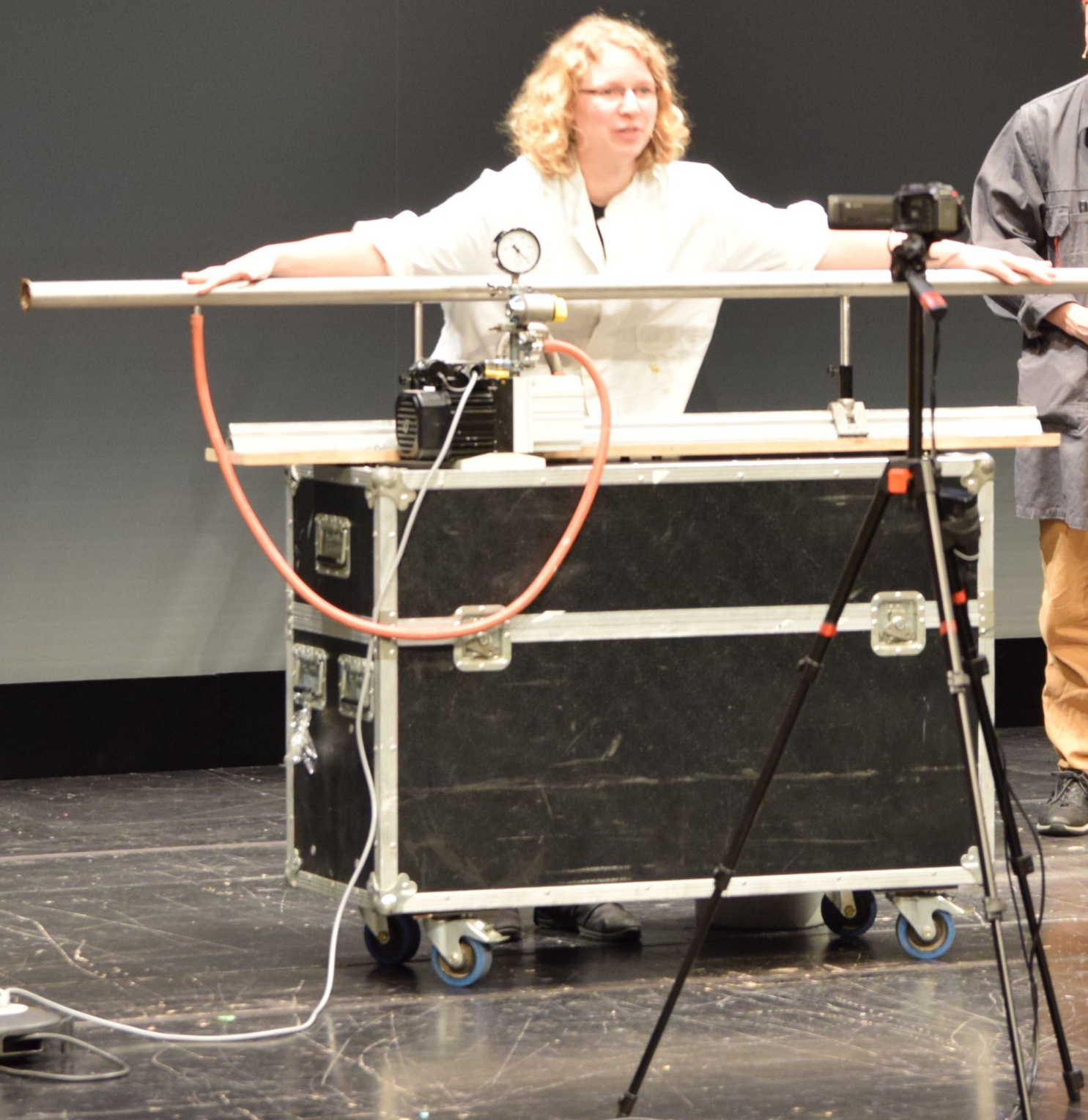




Particle Physics Show — Bonn University



Fund-



Roter Knopf:
Nicht drücken!
Niemals!









Roter Knopf:
Nicht drücken!
Niemals!





Fund-
sachen

Roter Knopf:
Nicht
drücken!
Niemand!

What's (the) Matter?

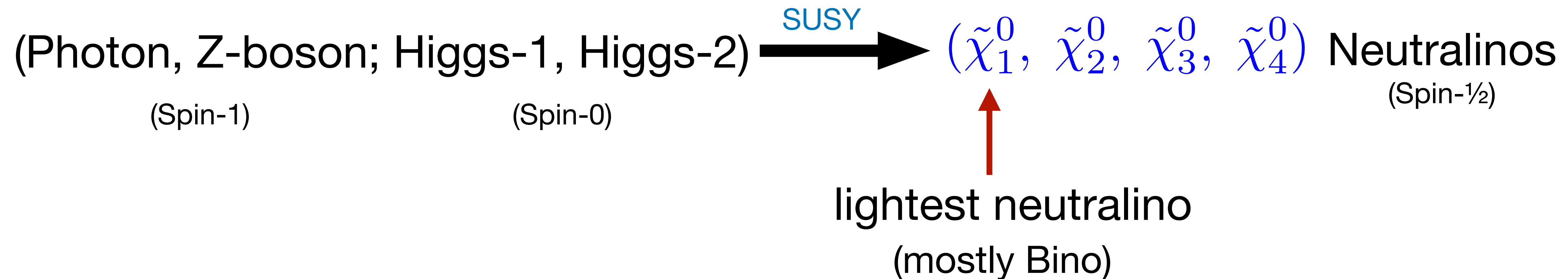
Die Teilchenphysik-Show

Prof. Herbert Dreiner und Studierende
der Rheinischen Friedrich-Wilhelms Universität Bonn

Einführung: Matthias Neubert, MITP Direktor



Light Long-Lived Particle: Supersymmetric Neutralino



Choudhury, HD, Richardson, Sarkar; *Phys.Rev.D* 61 (2000) 095009

Dedes, HD, Richardson; *Phys.Rev.D* 65 (2001) 015001

Light Neutralino: mass constraints

- LEP searches:

$$M_{\chi_1^0} \gtrsim 46 \text{ GeV}$$

- However, this is based on chargino searches, and assumption:

SUSY GUTs:

$$M_1 = \frac{5}{3} \tan^2 \theta_W M_2 \approx \frac{1}{2} M_2$$

- Drop assumption, and set determinant of neutralino mass matrix to 0

$$M_1 = \frac{M_2 M_Z^2 \sin(2\beta) \sin^2 \theta_W}{\mu M_2 - M_Z^2 \sin(2\beta) \cos^2 \theta_W}.$$

always
has
solutions

Light Neutralino: mass constraints

- Constraints: invisible Z-width
 - Radiative corrections
- } avoided, since
neutralino dominantly
bino

- Massless neutralino consistent with all constraints:

HKD, Heinemeyer, Kittel (Granada), Langenfeld, Weber, Weiglein: *Eur.Phys.J.C* 62 (2009) 547

- Strictest constraint from Supernova and White Dwarf cooling:

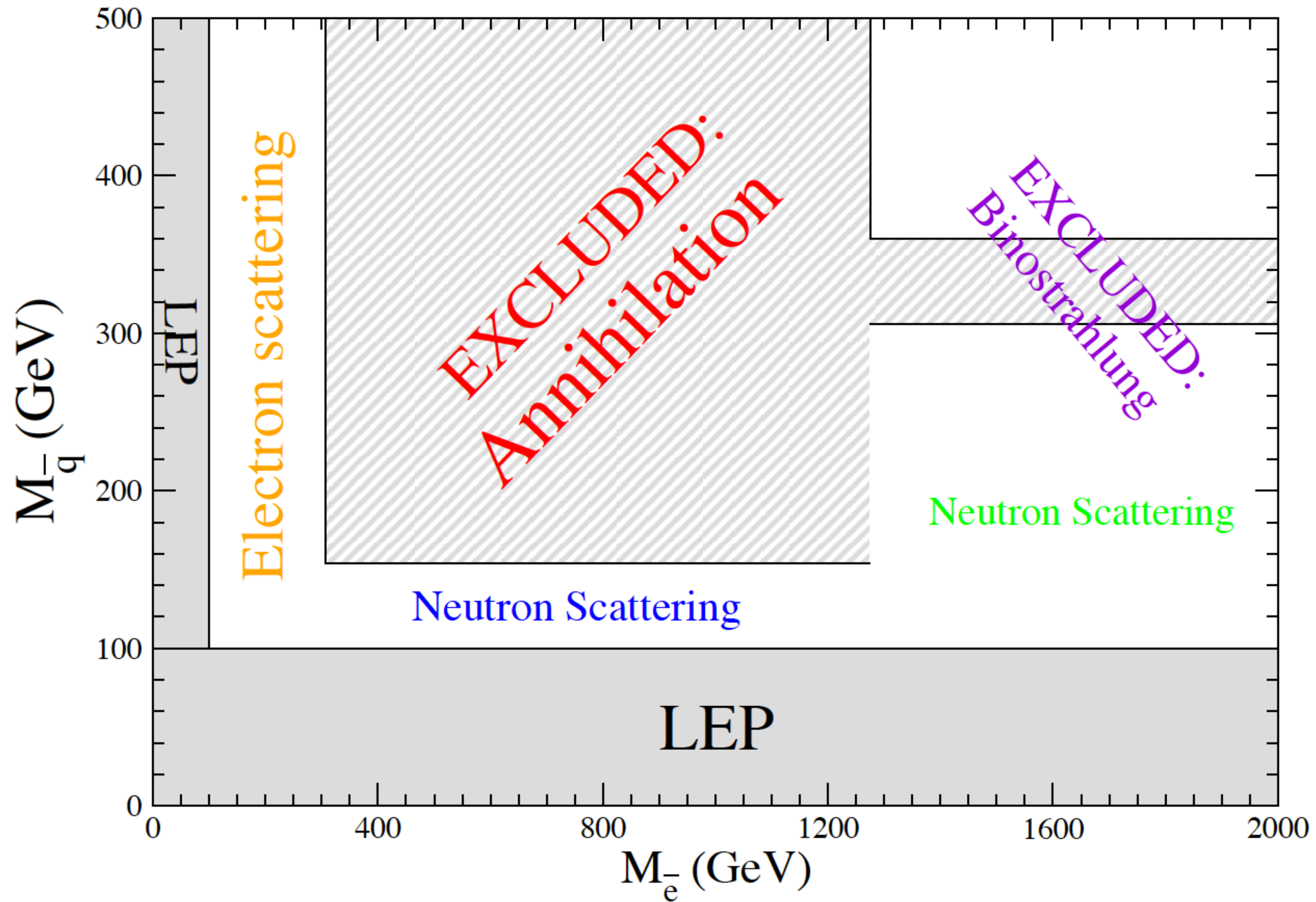
$$m_{\tilde{q}} > 600 \text{ GeV}$$

$$m_{\tilde{e}} > 1100 \text{ GeV}$$

C. Hanhart, HKD, et al: *Phys.Rev.D* 68 (2003) 055004

HKD, J. Fortin, L. Ubadi; *Phys.Rev.D* 88 (2013) 043517

Supernova Cooling Constraints



Cosmological Bounds

excluded for
stable $\tilde{\chi}_1^0$:

$$0.7 \text{ eV} < M_{\tilde{\chi}_1^0} < 24 \text{ GeV}$$

Cowsik-McClelland

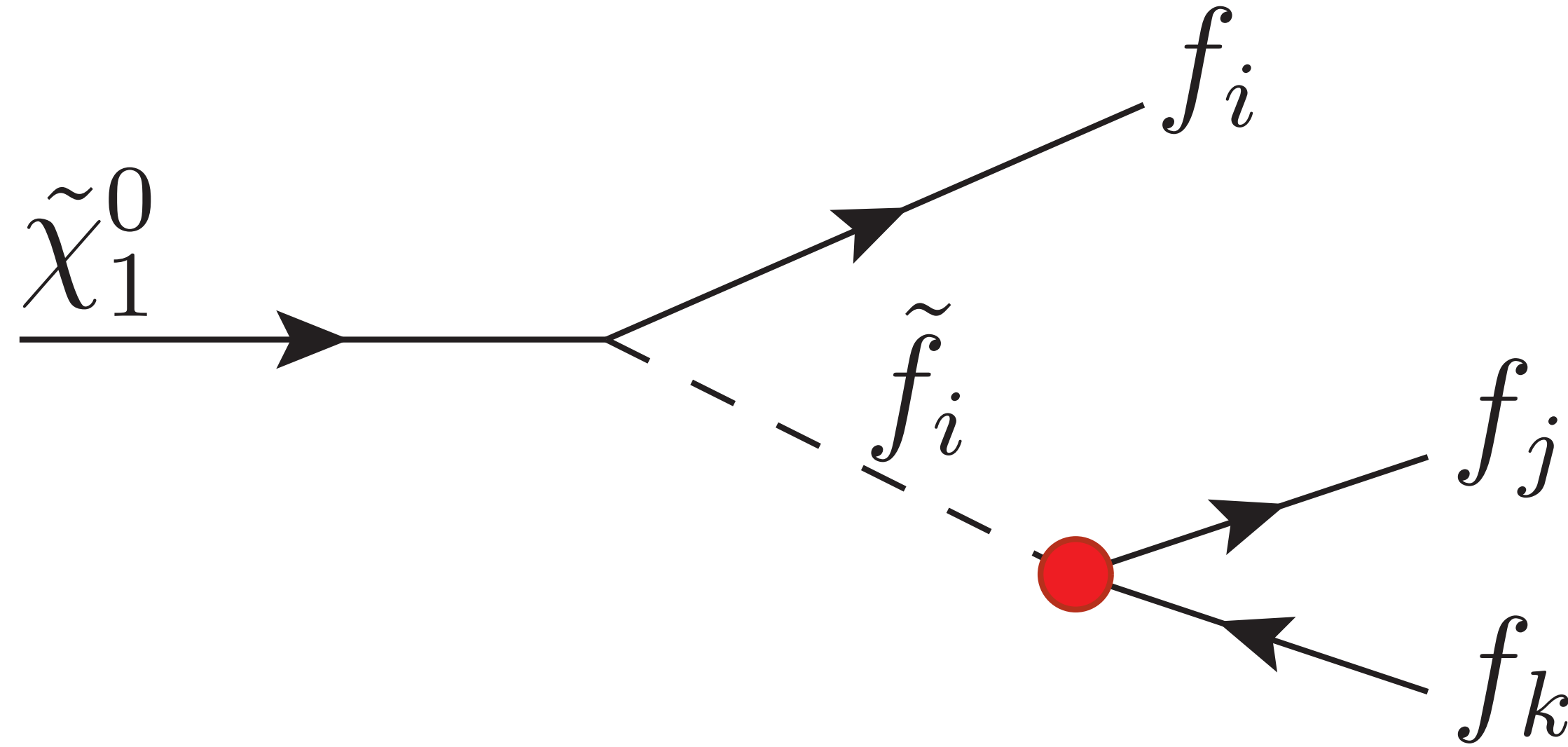
Lee-Weinberg

- In this range $\tilde{\chi}_1^0$ must decay, R-Parity Violation

$$W_{\text{RPV}} = \kappa_i L_i H_u + \lambda_{ijk} L_i L_j E_k^c + \lambda'_{ijk} L_i Q_j D_k^c + \lambda''_{ijk} U_i^c D_j^c D_k^c,$$

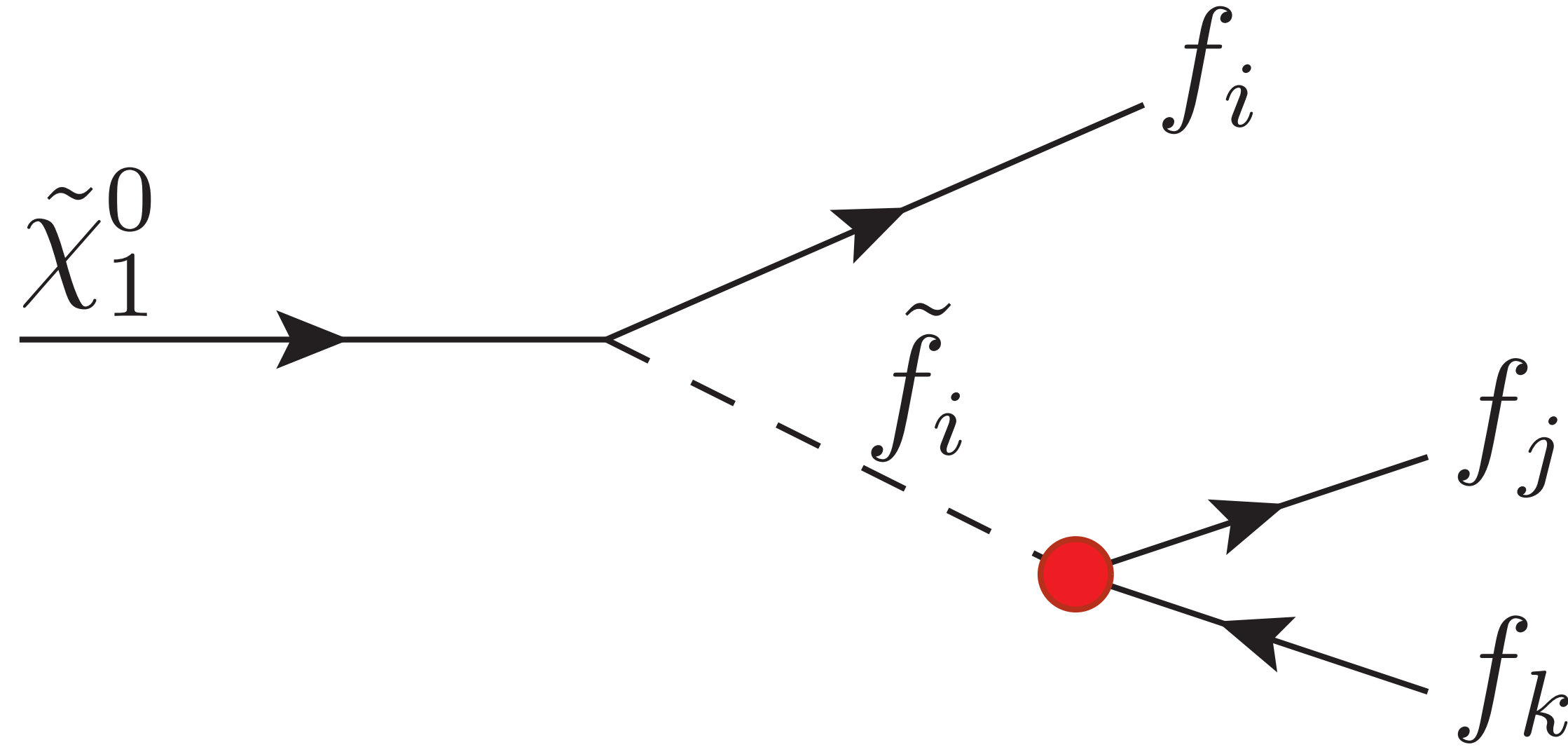
Neutralino no longer dark matter candidate — axino

LSP Decay – Heavy Neutralino



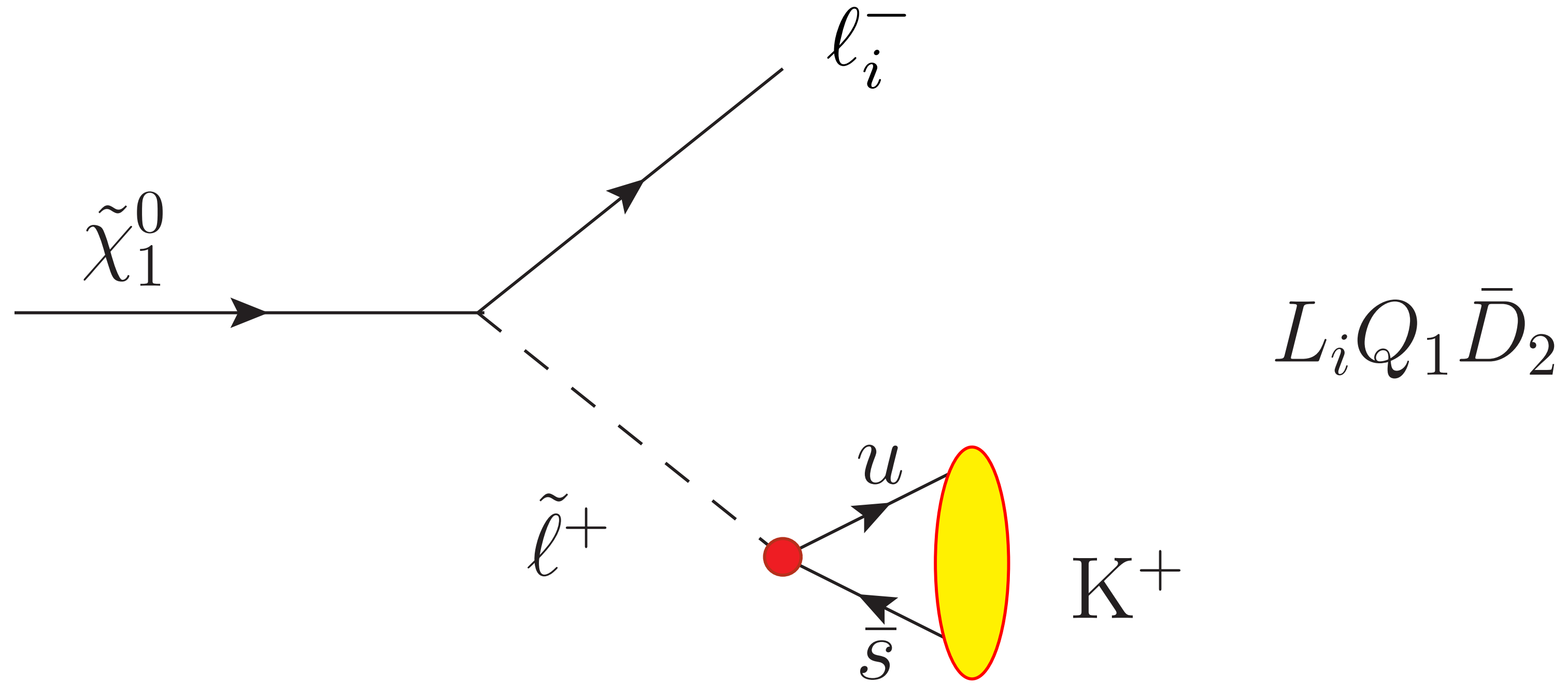
- UDD: 3 jets
- LQD: 2 jets + 1 lepton
- LLE: 2 charged leptons + 1 neutrino

LSP Decay – Lighter Neutralino



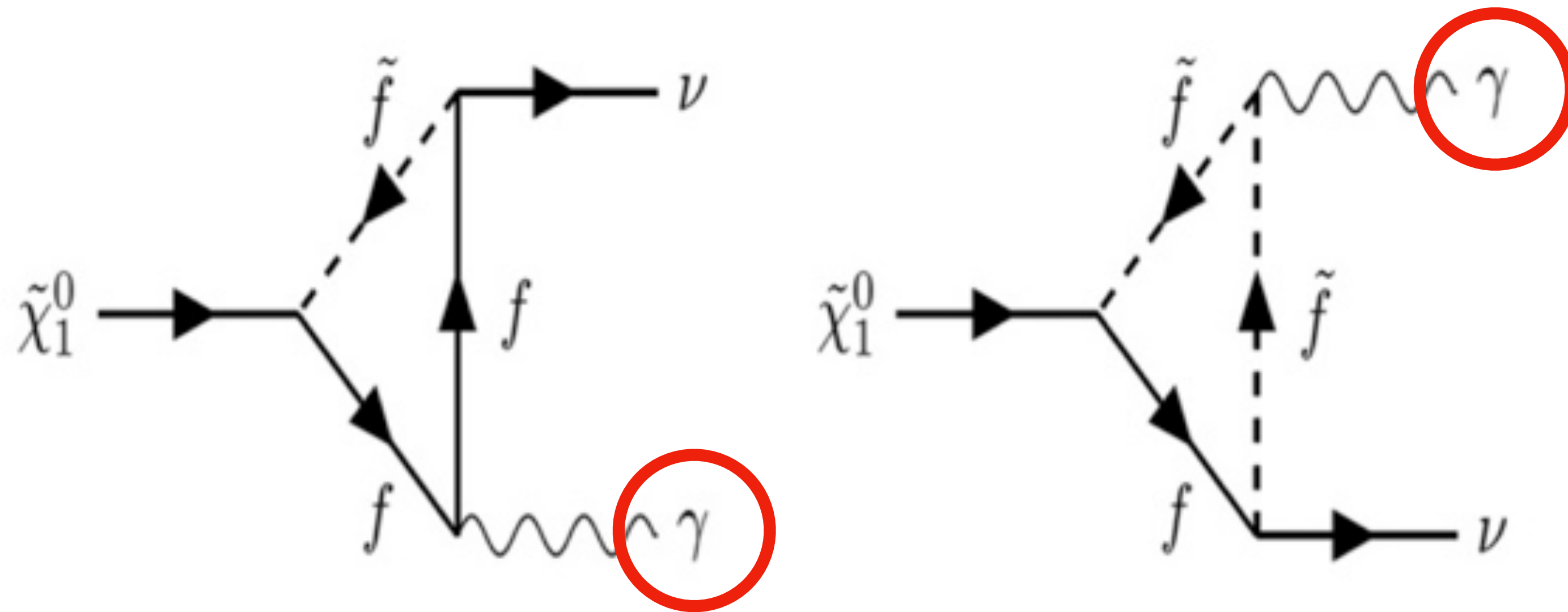
- UDD: ~~3 jets~~ baryon + meson
- LQD: ~~2 jets + 1 lepton~~ 1 meson + 1 lepton
- LLE: 2 charged leptons + 1 neutrino

LSP Decay – Lighter Neutralino



LSP Decay – Even Lighter Neutralino

$$\tilde{\chi}_1^0 \rightarrow \gamma + \nu$$



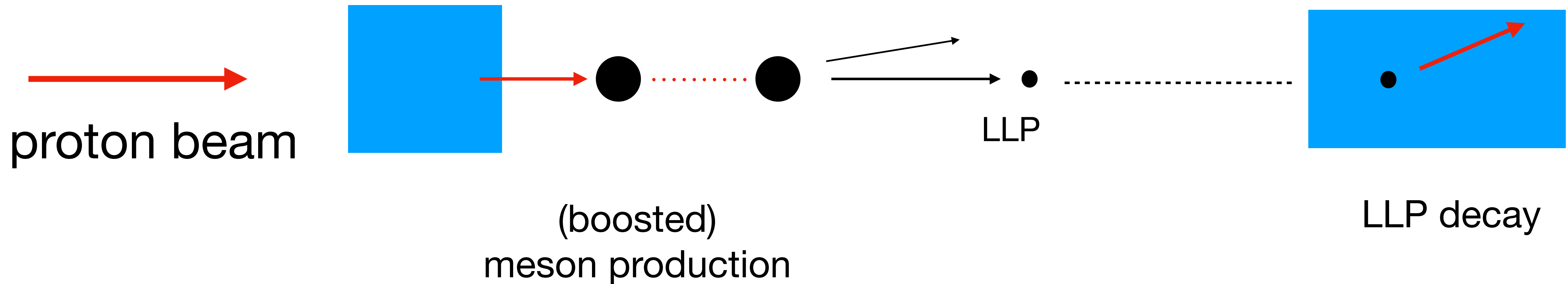
$$L_i L_j \bar{E}_j, \quad \text{or} \quad L_i Q_j \bar{D}_j$$

Light Long-Lived Particles (LLPs): 1. Colliders

Basic idea for detection:

hadronic collision
(collider, fixed-target)

rare meson
decay to LLP



FASER

Benchmark Scenarios for FASER

HD, Köhler, Nangia, Wang; *JHEP* 02 (2023) 120

$$\tilde{\chi}_1^0 \rightarrow \gamma + \nu$$

| Scenario | $m_{\tilde{\chi}_1^0}$ | Production (λ_{ijk}^P) | Decay (λ_{ijj}^D) | Current Constraints |
|-----------|------------------------|---|-----------------------------|--|
| B1 | 30 MeV | $\lambda'_{211} (M = \pi^\pm, \pi^0)$ | λ'_{333} | $\lambda'_{211} < 0.59 \left(\frac{m_{\tilde{d}_R}}{1 \text{ TeV}} \right), \lambda'_{333} < 1.04$ |
| B2 | 75 MeV | $\lambda'_{212} (M = K^\pm, K_{L/S}^0)$ | λ'_{333} | $\lambda'_{212} < 0.59 \left(\frac{m_{\tilde{s}_R}}{1 \text{ TeV}} \right), \lambda'_{333} < 1.04$ |
| B3 | 200 MeV | $\lambda'_{112} (M = K^\pm, K_{L/S}^0)$ | λ_{322} | $\lambda'_{112} < 0.21 \left(\frac{m_{\tilde{s}_R}}{1 \text{ TeV}} \right), \lambda_{322} < 0.7 \left(\frac{m_{\tilde{\mu}_R}}{1 \text{ TeV}} \right)$ |
| B4 | 300 MeV | $\lambda'_{221} (M = D^\pm, K_{L/S}^0)$ | λ_{233} | $\lambda'_{221} < 1.12, \lambda_{233} < 0.7 \left(\frac{m_{\tilde{\tau}_R}}{1 \text{ TeV}} \right)$ |
| B5 | 500 MeV | $\lambda'_{222} (M = D_S^\pm)$ | λ'_{222} | $\lambda'_{222} < 1.12$ |
| B6 | 1 GeV | $\lambda'_{313} (M = B^\pm, B^0)$ | λ'_{333} | $\lambda'_{313} < 1.12, \lambda'_{333} < 1.04$ |

Table 1. Benchmark scenarios considered in this paper. The neutralino is produced through the rare decay of the meson M via the coupling λ_{ijk}^P : $M \rightarrow \tilde{\chi}_1^0 + \ell (\nu)$. The neutralino decay is as in eq. (2.4) via the coupling λ_{ijj}^D . The photon energy in the neutralino rest frame is $E_\gamma = m_{\tilde{\chi}_1^0}/2$, but can range from $\mathcal{O}(0.1)$ to $\mathcal{O}(1)$ TeV at FASER. In the furthest-to-the-right column, we list the current best bounds on the couplings, see for example, ref. [38].

$$BR(\tilde{\chi}_1^0 \rightarrow \gamma + \nu)$$

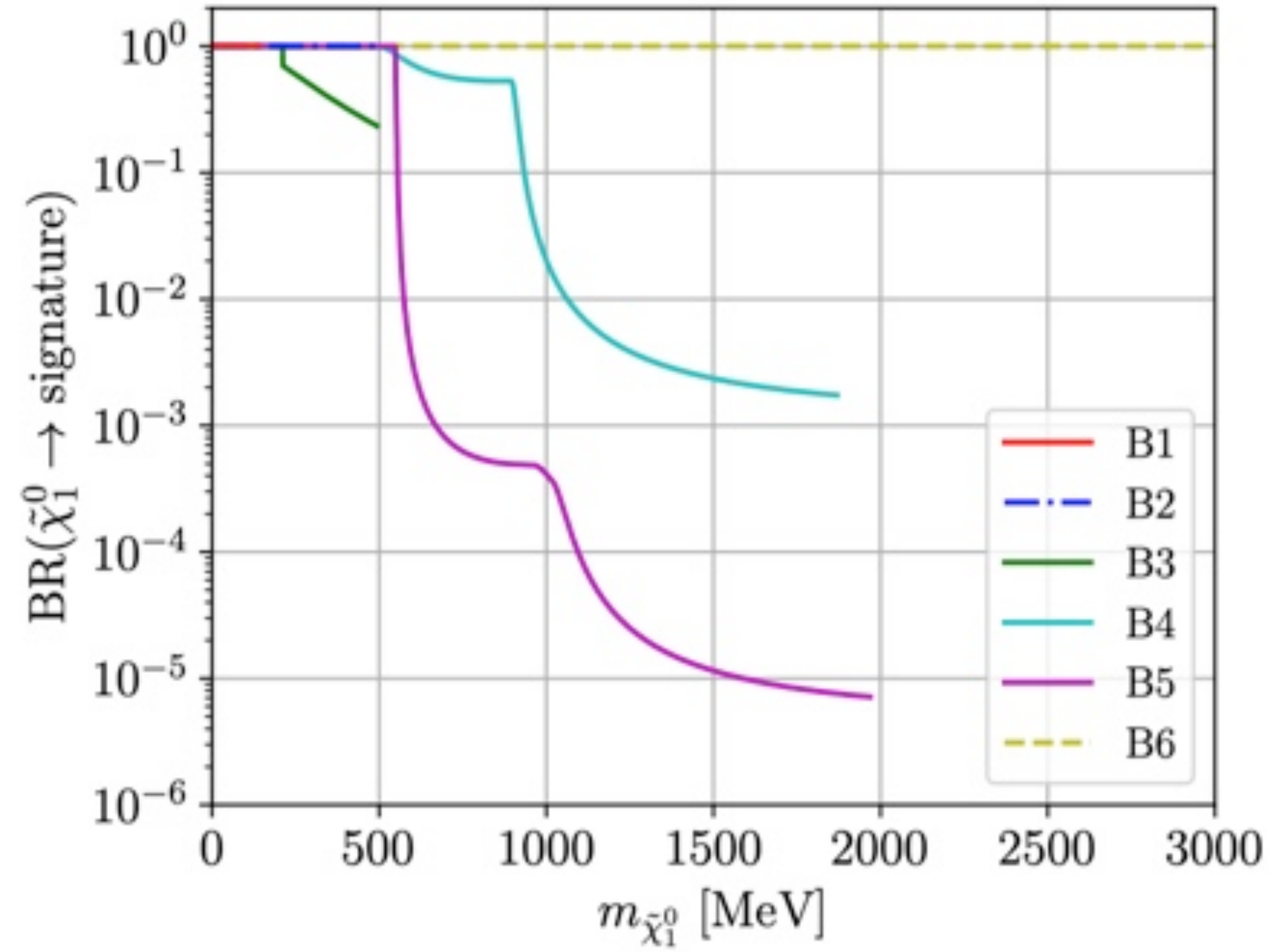


Figure 2. Branching ratios of the lightest neutralino into the single-photon signature, with varying neutralino mass.

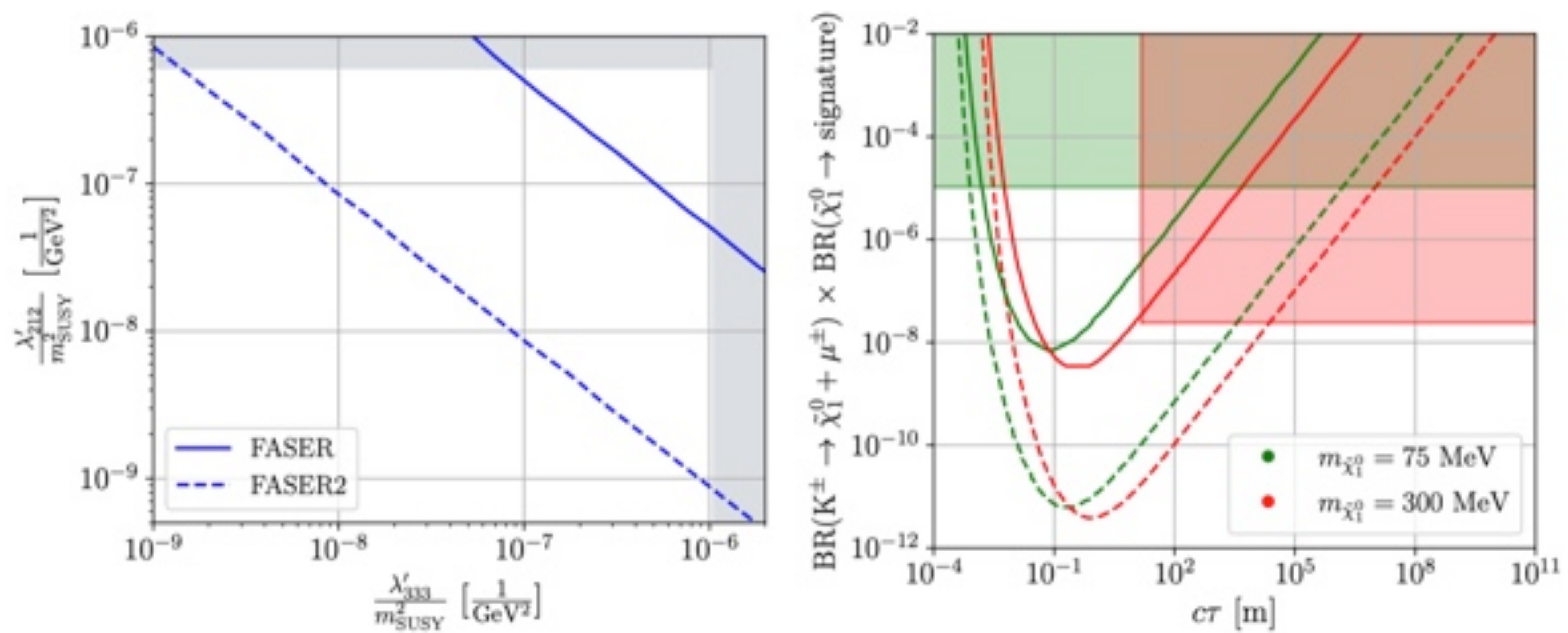
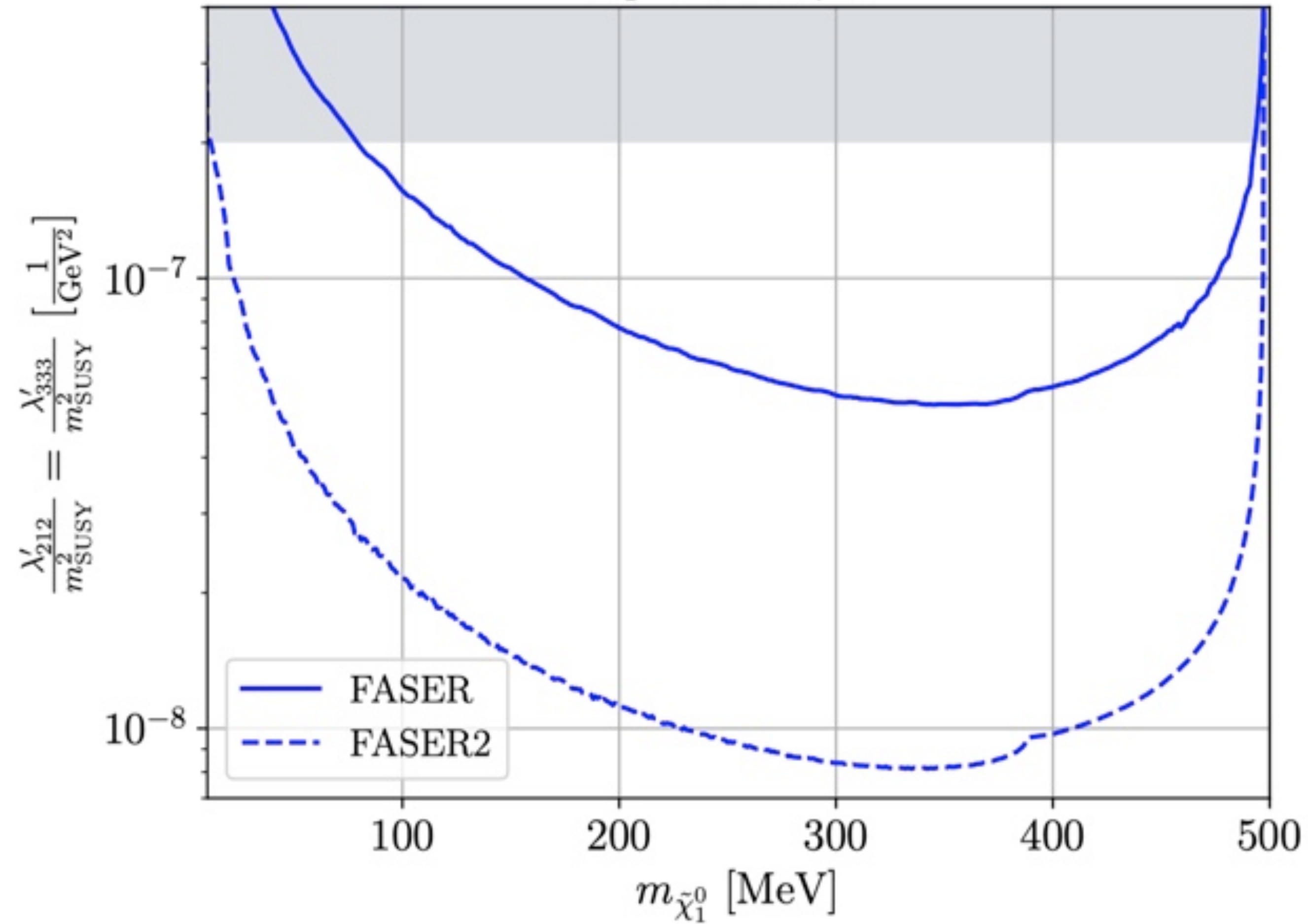


Figure 5. As in figure 3 but for the benchmark scenario **B2** with $m_{\tilde{\chi}_1^0} = 75$ MeV, *cf.* table 1. The right plot shows the sensitivity reach in $\text{BR}(K^\pm \rightarrow \tilde{\chi}_1^0 + \mu^\pm) \times \text{BR}(\tilde{\chi}_1^0 \rightarrow \text{signature})$ as a function of the neutralino decay length, $c\tau$, for $m_{\tilde{\chi}_1^0} = 75$ and 300 MeV.

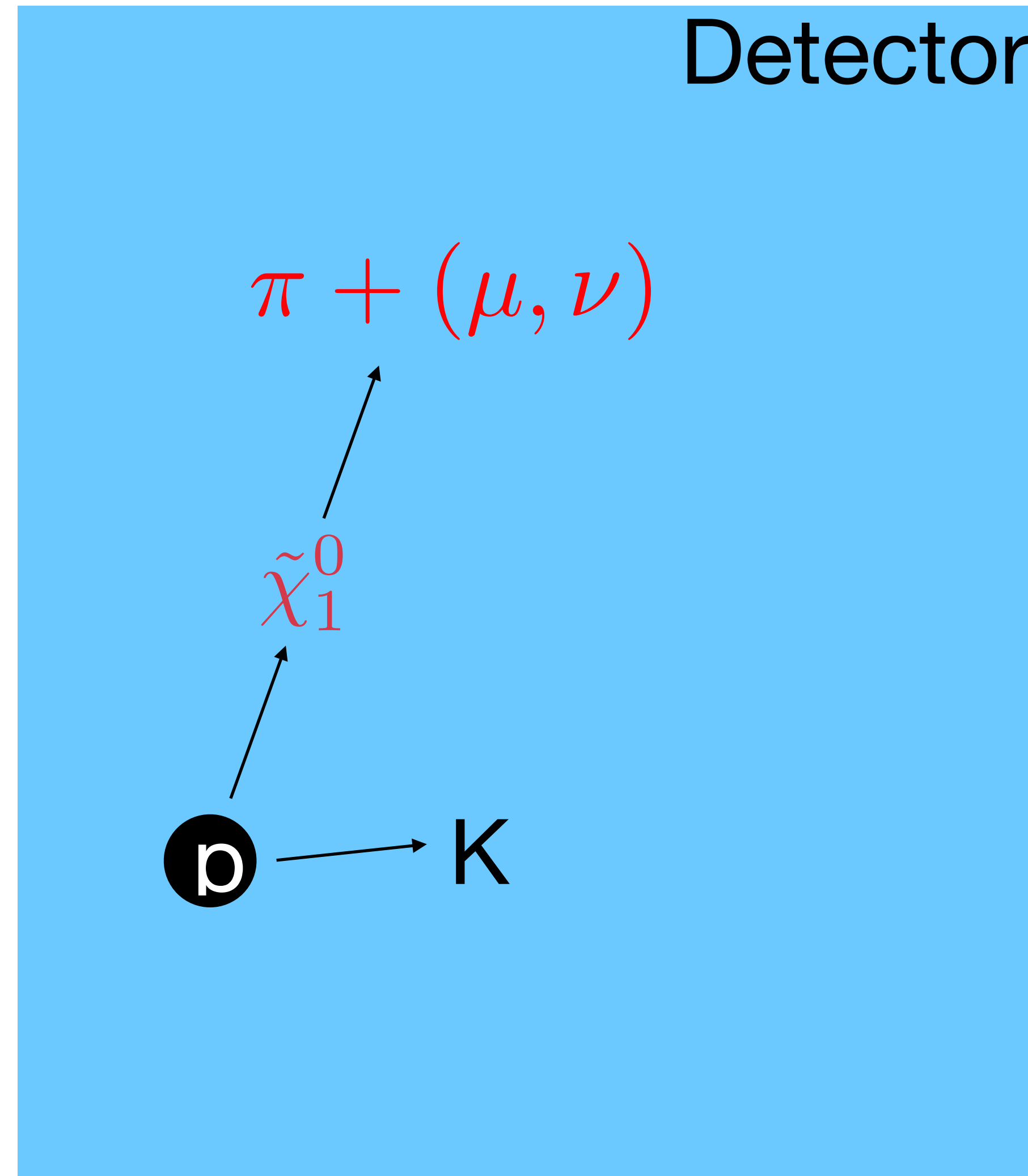
Benchmark 2

$$K^\pm / K^0 / \bar{K}^0 \rightarrow \tilde{\chi}_1^0 + \mu^\pm / \nu_\mu / \bar{\nu}_\mu$$
$$\tilde{\chi}_1^0 \rightarrow \gamma + \nu_\tau / \bar{\nu}_\tau$$



Proton Decay - Novel Decay Signature - Work in Progress

with: Cai-Dian Lü, Apoorva Shah, Saurabh Nangia, Dominik Köhler



$$\tilde{\chi}_1^0 \rightarrow \pi + (\mu, \nu)$$

$$\tilde{\chi}_1^0 \rightarrow \gamma + \nu$$

Upcoming Detectors

| | Super-K | Hyper-K | JUNO | DUNE |
|-------------------|--|--|------------------------------|--|
| Geometry | Cylindrical 42 m height × 39 m diameter | Cylindrical 60 m height × 74 m diameter | Spherical 35.4 m diameter | Cuboidal (4 modules) 58.2 m × 14 m × 12 m |
| Detector Material | Water | Water | LABs | Liquid Argon |
| Working Principle | Cherenkov | Cherenkov | Scintillation | Scintillation |
| Fiducial Mass | 22.5 kt | 187 kt | 20 kt | 40 kt |
| No. of Protons | $\sim 7.5 \times 10^{33}$ | $\sim 6.3 \times 10^{34}$ | $\sim 6.9 \times 10^{33}$ | $\sim 1.1 \times 10^{34}$ |
| $\epsilon_{inv.}$ | $\mathcal{O}(10)\%$ | $\mathcal{O}(10)\%$ | 37% | 30% |

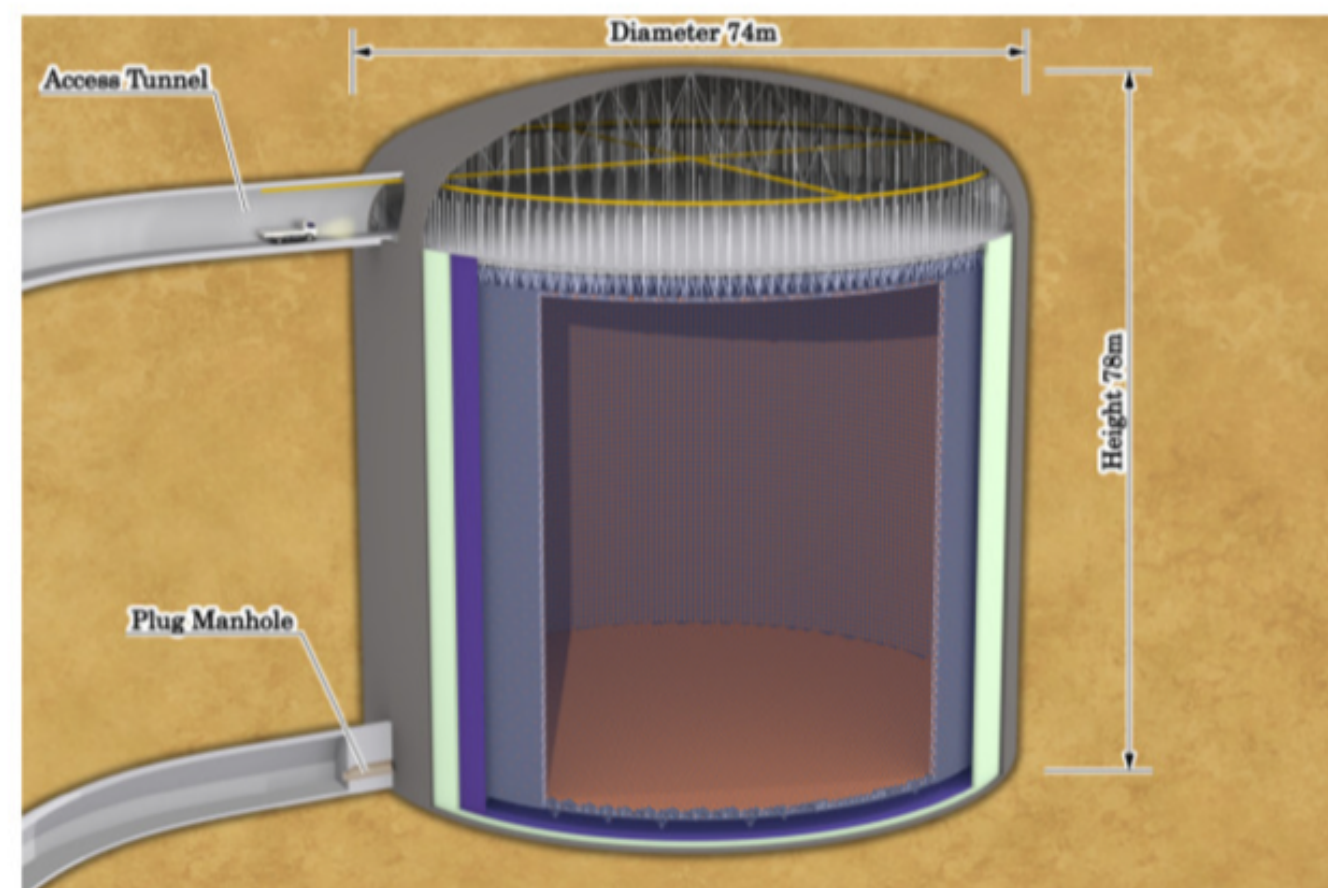


Figure 1: Hyper-K

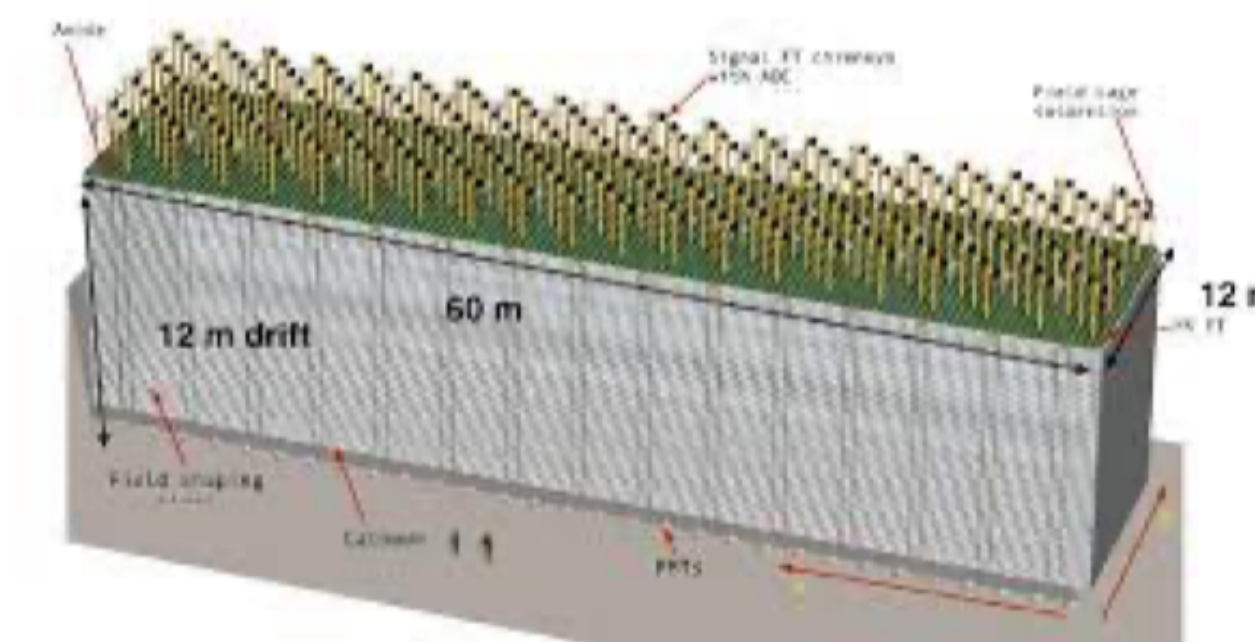


Figure 2: DUNE

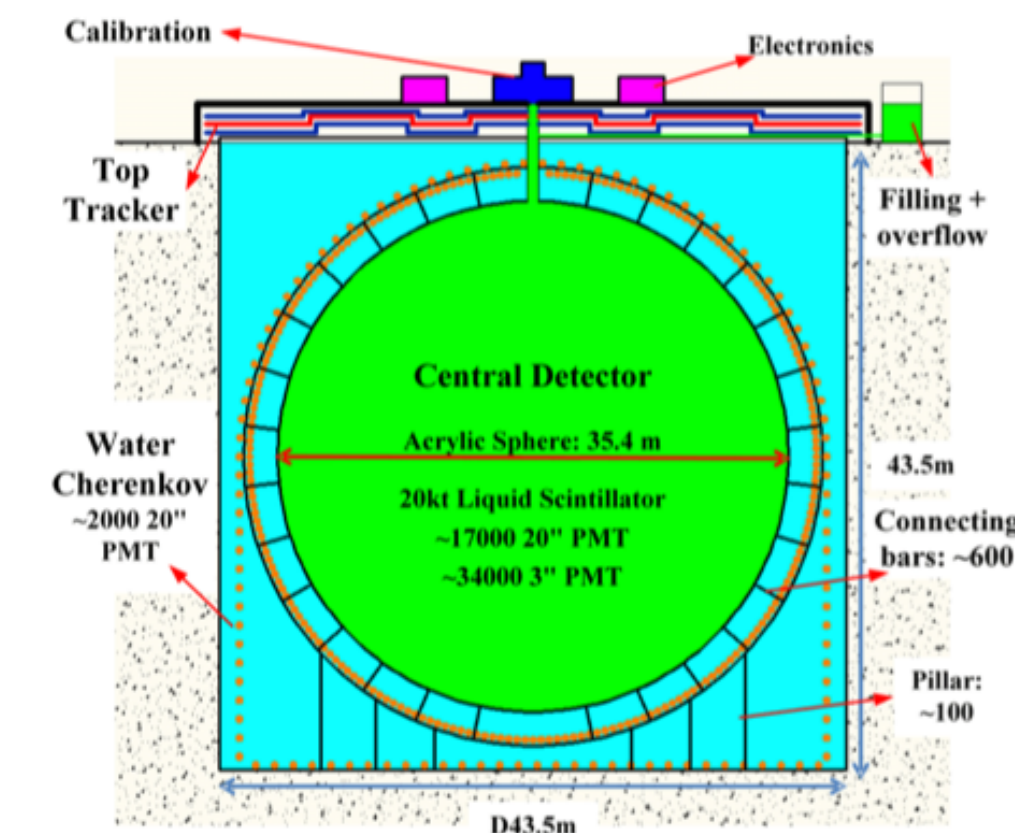


Figure 3: JUNO

includes
CAS

Benchmarks

| Scenario | $m_{\tilde{\chi}_1^0}$ | Proton Decay | $\tilde{\chi}_1^0$ Decay (λ_{ijk}^D) | Product Bound | Min. $c\tau_{\tilde{\chi}_1^0}$ |
|-----------|------------------------|--|--|--|---------------------------------|
| B1 | 0 – 400 MeV | $\lambda_{121}'' < 5 \times 10^{-7} \left(\frac{m_{\tilde{q}}}{\Lambda \text{TeV}} \right)^{5/2}$ | – | – | ∞ |
| B2 | 0 – 400 MeV | $\lambda_{121}'' < 5 \times 10^{-7} \left(\frac{m_{\tilde{q}}}{\Lambda \text{TeV}} \right)^{5/2}$ | $\lambda'_{333} < 1.04$ | $\lambda'_{333} \lambda_{121}'' < 10^{-9}$ | $\sim 1600 \text{ m}$ |
| B3 | 0 – 400 MeV | $\lambda_{121}'' < 5 \times 10^{-7} \left(\frac{m_{\tilde{q}}}{\Lambda \text{TeV}} \right)^{5/2}$ | $\lambda_{233} < 0.7 \left(\frac{m_{\tilde{\tau}_R}}{1 \text{TeV}} \right)$ | $\lambda_{233} \lambda_{121}'' < 10^{-21}$ | $\sim 180 \text{ m}$ |
| B4 | 150 – 400 MeV | $\lambda_{121}'' < 5 \times 10^{-7} \left(\frac{m_{\tilde{q}}}{\Lambda \text{TeV}} \right)^{5/2}$ | $\lambda'_{211} < 0.59 \left(\frac{m_{\tilde{d}_R}}{1 \text{TeV}} \right)$ | $\lambda'_{211} \lambda_{121}'' < 6 \times 10^{-25}$ | $\sim 11 \text{ m}$ |
| B5 | 150 – 400 MeV | $\lambda_{121}'' < 5 \times 10^{-7} \left(\frac{m_{\tilde{q}}}{\Lambda \text{TeV}} \right)^{5/2}$ | $\lambda'_{311} < 1.12$ | $\lambda'_{311} \lambda_{121}'' < 4 \times 10^{-24}$ | $\sim 30 \text{ m}$ |

} (rad)

$$\tilde{\chi}_1^0 \rightarrow \pi^\pm + \mu^\mp, \quad \pi^0 + \nu_\mu$$

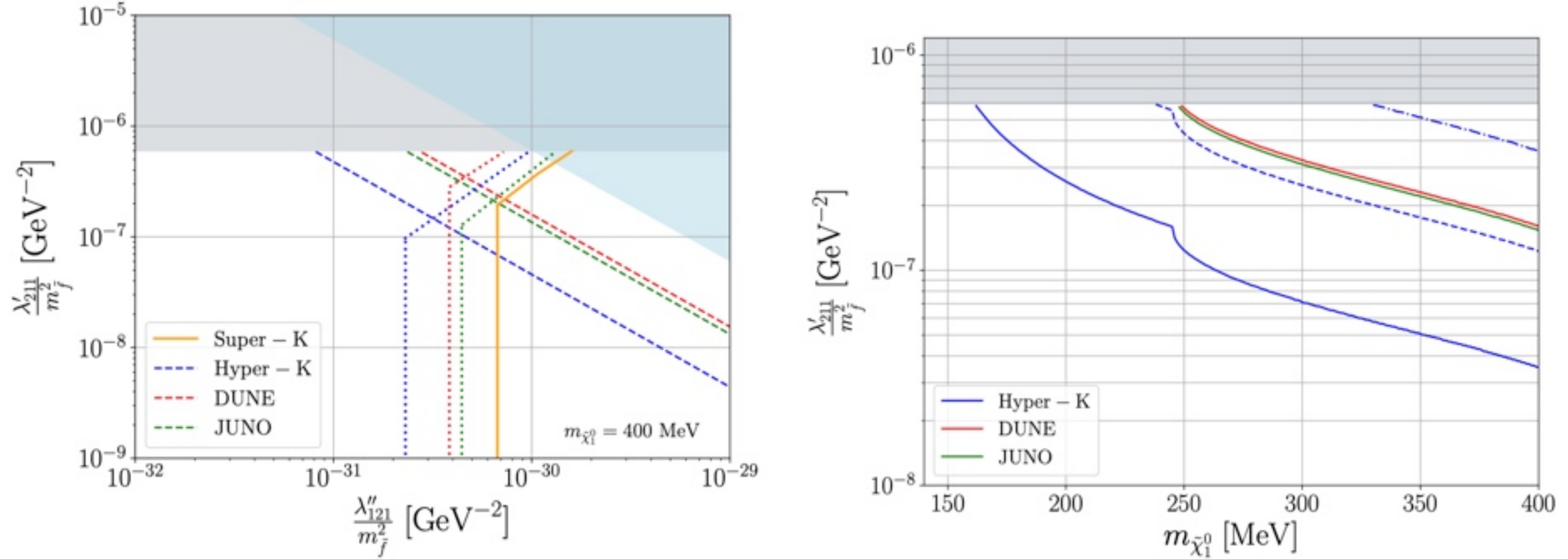


Figure 7: Sensitivity reach/Super-K limit for benchmark **B4**. The existing single-bound on λ'_{211} from Table 2 is shown in gray, the product-bound is in blue (both with $m_{\tilde{f}} = 1$ TeV), while the bound on λ''_{121} lies outside the scale of the plot. *Left:* As in left plot of Fig. 5 but for benchmark **B4**. *Right:* As in right plot of Fig. 4 but for benchmark **B4**. The solid, dashed, and dot-dashed lines correspond to 3-, 30- and 90-event isocurves, respectively.

P.S.

Completing 2nd book: Popular Physics Book

Faszinierende Teilchenphysik

Springer Verlag

Co-Authors: Philip Bechtle (Bonn)

Florian Bernlochner (Bonn)

Josef Jochum (Tübingen)

Christoph Hanhart (FZ Jülich, Bonn)

Jörg Pretz (Aachen, FZ Jülich)